



# A high voltage magnesium battery based on H<sub>2</sub>SO<sub>4</sub>-doped (PVA)<sub>0.7</sub>(NaBr)<sub>0.3</sub> solid polymer electrolyte

E. Sheha\*, M.K. El-Mansy

Physics Department, Faculty of Science, Benha University, Benha, Egypt

## ARTICLE INFO

### Article history:

Received 8 July 2008

Received in revised form 17 August 2008

Accepted 10 September 2008

Available online 24 September 2008

### Keywords:

Solid polymer electrolyte  
Ionic conductivity  
Dielectric properties  
Magnesium battery

## ABSTRACT

Solid polymer electrolytes (SPE) based on poly (vinyl alcohol) (PVA) and sodium bromide (NaBr) complexed with sulfuric acid (SA) at different weight percent ratios were prepared using solution cast technique. The structural properties of these electrolyte films were examined by XRD studies. The XRD data revealed that sulfuric acid disrupt the semi-crystalline nature of (PVA)<sub>0.7</sub>(NaBr)<sub>0.3</sub> and convert it into an amorphous phase. AC conductivity and dielectric spectra of the electrolyte were studied with changing sulfuric acid content from 0.87 to 3.4 moles l<sup>-1</sup> (M). The highest conductivity of (PVA)<sub>0.7</sub>(NaBr)<sub>0.3</sub> matrix at room temperature was  $1.12 \times 10^{-6} \text{ S cm}^{-1}$  and this increased to  $6 \times 10^{-4} \text{ S cm}^{-1}$  with doping by 2.6 M sulfuric acid. The electrical conductivity ( $\sigma$ ) and dielectric permittivity ( $\epsilon'$ ) of the solid polymer electrolyte in frequency range (100 Hz to 100 kHz) and temperature range (300–400 K) were carried out. The electrolyte with the highest electrical conductivity was used in the fabrication of a magnesium battery with the configuration Mg/SPE/MnO<sub>2</sub>. The fabricated cells give capacities of 4.85 mAhg<sup>-1</sup> and have an internal resistance of 900  $\Omega$ .

© 2008 Elsevier B.V. All rights reserved.

## 1. Introduction

In view of negligible hazards and enhanced safety, studies on rechargeable magnesium batteries are expected to have a wide scope in the future. Magnesium metal possesses a number of characteristics which make it attractive as a negative electrode material for rechargeable batteries; highly negative standard potential (−2.375 V versus SHE), relatively low equivalent weight (12 g Faraday<sup>-1</sup>), high melting point (649 °C), low cost, relative abundance, high safety, ease of handling, and low toxicity which allows for urban waste disposal [1–3].

Studies on the electrical properties of polymer electrolyte have attracted much attention in view of their application in electronic devices like fuel cells, solar cells and solid-state batteries. Electrical conduction in polymers has been studied aiming to understand the nature of the charge transport prevalent in these materials. The electrical properties of polymer can be suitably modified by the addition of dopants. Poly (vinyl alcohol) (PVA) is an exceptional polymer; PVA is a potential material having high dielectric strength, good charge storage capacity and dopant-dependent electrical and optical properties. It has a carbon chain backbone with hydroxyl

groups attached to methane carbons. These OH-groups can be a source of hydrogen bonding and hence assist the formation of polymer electrolytes [4–9]. Rao and co-workers [6] have a solid polymer electrolyte (SPE) development of PVA complexed with NaBr systems. They have got the conductivity of up to  $1.12 \times 10^{-6} \text{ S cm}^{-1}$ , from PVA:NaBr wt.% ratio of 70:30.

Sulfuric acid (SA) H<sub>2</sub>SO<sub>4</sub>, is a strong mineral acid has a high electrical conductivity due to an intra-molecular proton-switch mechanism, its incorporation in a polymer system may be expected to enhance its electrical performance [9]. We propose to develop a radically new, alternative ionic-conducting electrolyte (or membrane) that is based on compounds whose chemistry and properties are intermediate between those of a normal acid, such as H<sub>2</sub>SO<sub>4</sub>, and a normal salt, such as NaBr and not a hydrated polymer. Thus, composite membranes will be developed, in which a solid acid is embedded in an inert polymer matrix, with the polymer providing mechanical support and enhancing chemical stability. Hence the current work is aimed at improving the electrical and electrochemical properties of (PVA)<sub>0.7</sub>(NaBr)<sub>0.3</sub> through doping in different proportions of sulfuric acid. Structure and ionic conductivity studies are performed on the solid polymer electrolyte. With a SPE of optimum composition, solid-state Mg/SPE/MnO<sub>2</sub> cell is assembled, and its cycling performances will be briefly examined to evaluate the applicability of the solid polymer electrolyte to solid-state magnesium batteries.

\* Corresponding author. Tel.: +20 10741 4705; fax: +20 133222 578.  
E-mail address: [e.sheha@yahoo.com](mailto:e.sheha@yahoo.com) (E. Sheha).

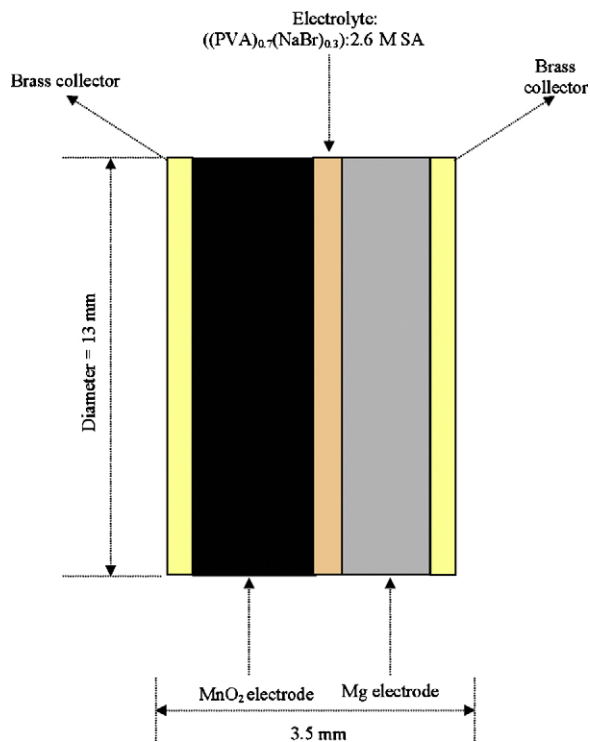


Fig. 1. Mg/polymer electrolyte/MnO<sub>2</sub> cell.

## 2. Experimental

### 2.1. Preparation of SPE

PVA with molecular weight  $\sim 1800$  was obtained from QualiKems chemical company (India). The PVA-based membranes were prepared by dissolving 0.7 g of PVA in distilled water, to get a 10 wt.% solution. The solution was left for 24 h at 50 °C in order to obtain a transparent low-viscous liquid. At this point approximately 0.3 g of NaBr (SIGMA) was added to the solution. The solution was left to stir for 20 min. Then  $xM$  ( $x = 0.87, 1.7, 2.6$  and  $3.4 M$ ) of H<sub>2</sub>SO<sub>4</sub> (GPR-

ADWIC) solution was gradually added to the beaker. The solution was left to stir for 24 h. The transparent solution was then cast on a Petri-glass dish for 2 weeks. The final product was vacuum dried thoroughly.

### 2.2. Characterization

In order to investigate the nature of these polymer electrolyte films, X-ray diffraction studies were carried out using Bruker X-ray diffractometer. The diffraction system based with Cu tube anode of wave length  $K_{\alpha 1} = 1.5460 \text{ \AA}$  and  $K_{\alpha 2} = 1.54439 \text{ \AA}$ . The start angle ( $2\theta$ ) was 4° and the end angle was 50°.

Samples of diameter 1 cm were taken and silver was deposited on both surfaces of the film to ensure good contacts in electrical measurements. Silver coated samples were sandwiched between the two similar brass electrodes of a spring-loaded sample holder. The whole assembly was placed in a furnace monitored by a temperature controller. The rate of heating was adjusted to be  $2 \text{ K min}^{-1}$ . Dielectric and electrical measurements were carried out in the temperature range 303–373 K using PM 6304 programmable automatic RCL (Philips) meter. The measurements were carried out over a frequency range 100 Hz to 100 kHz.

### 2.3. Mg/SPE/MnO<sub>2</sub> cell

Magnesium battery was fabricated from the film PVA–NaBr– $xM$  (SA) that gave the highest electrical conductivity. 0.4 g  $\gamma$ -MnO<sub>2</sub> powder (domestic source) and 0.1 g of graphite (QualiKems) powder were mixed with 10% PVA solution as binder to form an cathode pellet of the battery, while 0.25 g magnesium powder (Aldrich) was used to form the anode pellet. A hydraulic press ( $2 \text{ tons cm}^{-2}$ ) was used to compress the pellets. The cells were then assembled by sandwiching the SPE between the two electrodes, Fig. 1. The open-circuit voltage (OCV) was measured for the batteries stored at an open-circuit condition for 24 h. The discharge characteristics of the cell were monitored under a constant load of 100 k $\Omega$ . Current drains ranging from 20 to 500  $\mu\text{A}$  were used to plot the current–voltage ( $I$ – $V$ ) and current density–power density ( $J$ – $P$ ) curves. The average of each battery's voltage was monitored for each current drain after 10 s of operation. The internal resistance of the cell was then

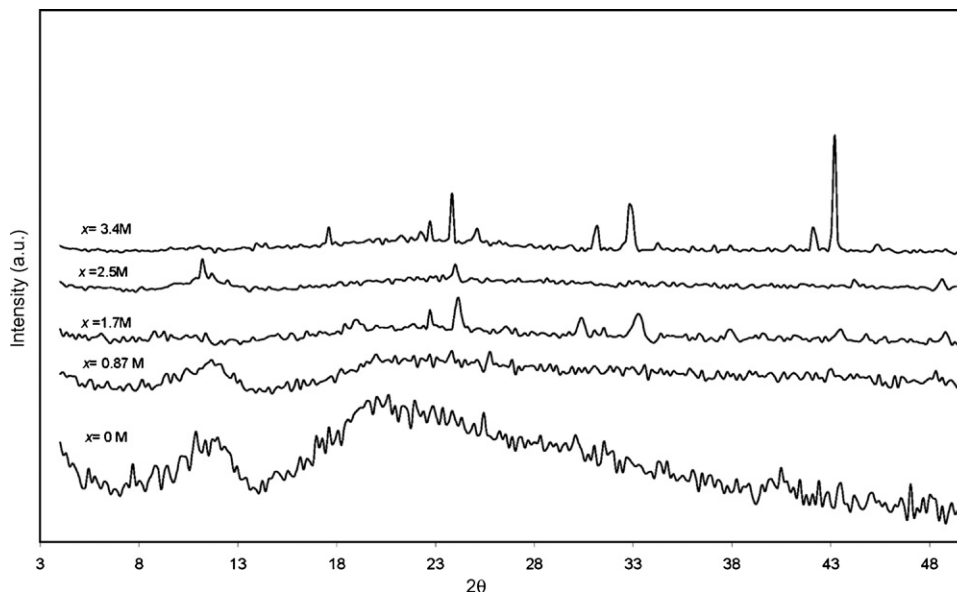


Fig. 2. XRD pattern of (PVA)<sub>0.7</sub>(NaBr)<sub>0.3</sub>: $xM$  (SA) polymer electrolyte.

calculated by using equation:

$$V = E - Ir$$

where  $V$  is the voltage,  $E$  the electromotive force,  $I$  the current and  $r$  is the internal resistance.

### 3. Results and discussion

#### 3.1. XRD analysis

The crystallinity of the polymer film with respect to pure and  $\text{H}_2\text{SO}_4$  (SA)-doped  $(\text{PVA})_{0.7}(\text{NaBr})_{0.3}$  complexes has been examined by X-ray diffraction. The diffraction pattern for pure  $(\text{PVA})_{0.7}(\text{NaBr})_{0.3}$  is shown in Fig. 2. The sample is partially crystalline with a broad peak at  $2\theta = 19.5^\circ$ . The broad peak becomes less intense as the SA content is increased to up to 2.6 M. This could be due to the disruption of the  $(\text{PVA})_{0.7}(\text{NaBr})_{0.3}$  semi-crystalline structure by SA. XRD shows that the sample with  $(\text{PVA})_{0.7}(\text{NaBr})_{0.3}:2.6\text{ M SA}$  is the least crystalline as shown in Fig. 2. In the film with 3.4 M SA, Fig. 2, the peaks at  $2\theta = 33^\circ$  and  $44^\circ$  can be attributed to some crystalline phases due to high concentration of  $\text{H}_2\text{SO}_4$ .

#### 3.2. AC conductivity studies

The conductivity of pure  $(\text{PVA})_{0.7}(\text{NaBr})_{0.3}$  is  $\approx 10^{-6}\text{ S cm}^{-1}$  [6] and it increases sharply to  $\approx 10^{-4}\text{ S cm}^{-1}$  on complexing the  $(\text{PVA})_{0.7}(\text{NaBr})_{0.3}$  with SA. Fig. 3 shows the variation of conductivity  $\sigma$  with the amount of SA added. It can be seen that the conductivity increases with the amount of SA added up to 2.6 M after which the conductivity decreases. The results depicted in Fig. 3 seem to agree with the results obtained from XRD analysis. The degree of crystallinity affects the electrical conductivity of the samples. The amorphous nature produces greater ionic diffusivity in accordance with the high ionic conductivity, which can be obtained in amorphous polymers that have a fully flexible backbone [10]. On further addition of SA to 3.4 M, the conductivity begins to decrease. This is attributed to the crystallinity of the sample as indicated by XRD.

We have attempted to explain the variation in conductivity with SA content in terms of the preparation of the films, where different amounts of SA were added to each solution. Hence, the volume of the host matrix  $((\text{PVA})_{0.7}(\text{NaBr})_{0.3})$  was the same for all films. Two characteristic regions can be easily distinguished. The initial low concentration region (I) in which an increase in conductivity is observed has been attributed to triple ion formation or re-dissociation effect [11]. The second high concentration region (II) in which more and more SA was added, the host matrix became more crowded with dopant ions. Such overcrowding reduces the

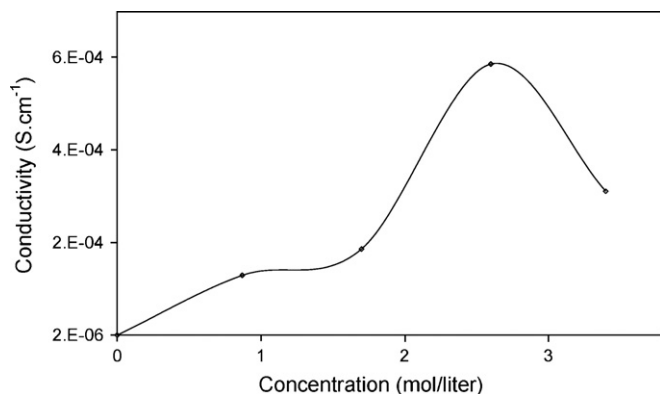


Fig. 3. Variation of ionic conductivity of  $(\text{PVA})_{0.7}(\text{NaBr})_{0.3}:x\text{ M SA}$  polymer electrolyte system as a function of SA concentration.

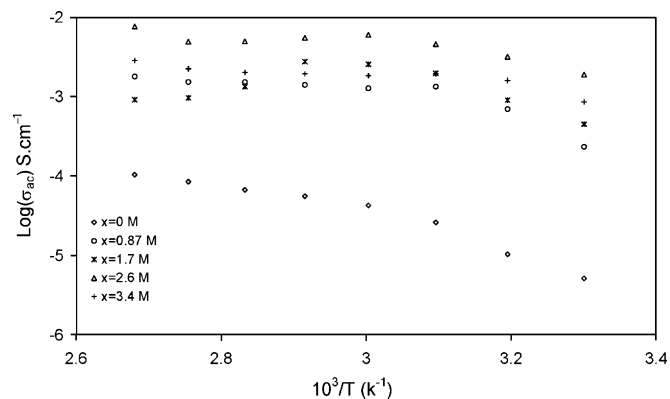


Fig. 4. Temperature dependent conductivity at 10 kHz of  $(\text{PVA})_{0.7}(\text{NaBr})_{0.3}:x\text{ M SA}$  polymer electrolyte.

number of charge carriers due to the limitation of ionic mobility. Thus, the conductivity decreases after 2.6 M SA [12].

Fig. 4 represents the temperature dependence of ionic conductivity for all compositions of  $((\text{PVA})_{0.7}(\text{NaBr})_{0.3}):x\text{ M SA}$  polymer electrolytes at frequency 10 kHz. The temperature dependence of conductivity of polymer electrolytes follows many patterns, as widely discussed by Ratner [7]. However, in the present study the plot shows two kinds of patterns:

1. For the PVA:NaBr:SA system containing low SA concentration, the ionic conductivity of the membranes increases with increasing temperature but with two regions (region I and region II) with different activation energies, indicating Arrhenius type thermally activated process given by the relation.

$$\sigma_{ac} = \sigma_0 \exp\left(\frac{-E_a}{k_B T}\right)$$

where  $\sigma_0$  is the pre-exponential factor,  $E_a$  the activation energy and  $k$  is the Boltzmann constant.

2. For the PVA:NaBr:SA system containing high SA concentration, the ionic conductivity of the membranes increases with increasing temperature through the first region. While, the second region follows the liquid-like behavior. Thus, as the addition of SA increased, the conductivity behavior changed from Arrhenius to liquid-like behavior [7].

The calculated activation energies (combination of the energy of defect formation and the energy for migration of ion) as a function of SA concentration in the polymer electrolyte are listed in Table 1. It has been found that the highest conductivity polymer electrolyte (PVA:NaBr:2.5 M SA) has the lowest activation energy (0.41 eV). It is noteworthy that the polymer electrolytes with low values of activation energies are desirable for practical applications.

Druger et al. [8] have attributed the increase in conductivity with temperature in solid polymer electrolyte to segmental (i.e. polymer

Table 1

Activation energies ( $E_a$ ), and conduction index ( $n$ ) values of  $(\text{PVA})_{0.7}(\text{NaBr})_{0.3}:x\text{ M SA}$  polymer electrolyte films.

x M (SA)	Activation energy		n
	Region I	Region II	
0	0.68	0.23	0.05
0.87	0.83	0.16	0.11
1.7	0.67	–	0.13
2.6	0.41	–	0.22
3.4	0.48	–	0.22

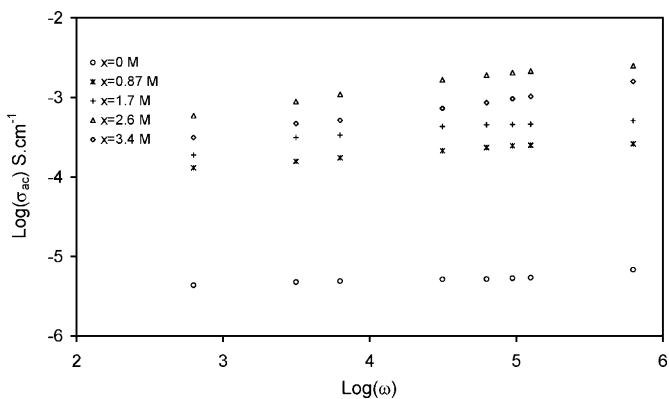


Fig. 5. Frequency dependent conductivity at 303 K of (PVA)<sub>0.7</sub>(NaBr)<sub>0.3</sub>:x M (SA) polymer electrolyte.

chain) motion, which results in an increase in the free volume of the system. Thus, the segmental motion either permits the ions to hop from one site to another or provides a pathway for ions to move. In other words, the segmental movement of the polymer facilitates the translational ionic motion. From this, it is clear that the ionic motion is due to translational motion/hopping facilitated by the dynamic segmental motion of the polymer. As the amorphous region increases the polymer chain acquires faster internal modes in which bond rotations produce segmental motion to favor inter- and intra-chain ion hopping, and thus the degree of conductivity becomes high.

The variation of AC conductivity with frequency for different concentrations of SA-doped (PVA)<sub>0.7</sub>(NaBr)<sub>0.3</sub> at 303 K is shown in Fig. 5. The AC conductivity  $\sigma_{ac}$  shows little increase with frequency obeying the power relation [13]:

$$\sigma_{ac} \propto \omega^n$$

where  $\omega$  is the angular frequency and  $n$  is the index which is characteristic of the type of conduction mechanism/relaxation mechanism dominant in amorphous materials. The value of  $n$  evaluated from Fig. 5 to (PVA)<sub>0.7</sub>(NaBr)<sub>0.3</sub> is around 0.05 both at lower and higher temperatures. The calculated values of  $n$  as a function of SA concentration in the polymer electrolyte are listed in Table 1. It can be seen that the value of  $n$  increases with the amount of SA added. This behavior can be interpreted in light of the fact that doping of sulfuric acid increases the number of chain segments that are responsive to the external electric field frequency.

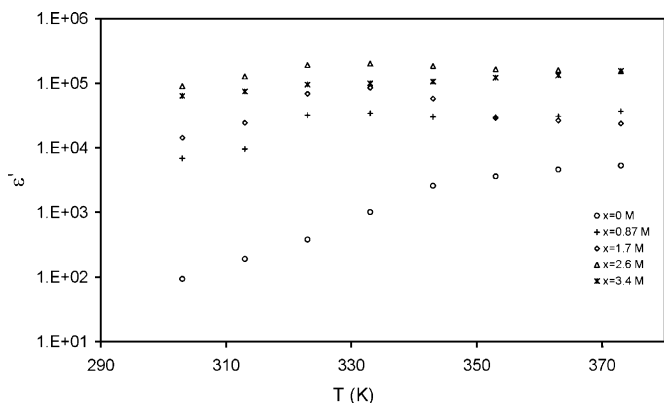


Fig. 6. Variation of dielectric constant with temperature at frequency 10 kHz of (PVA)<sub>0.7</sub>(NaBr)<sub>0.3</sub>:x M (SA) polymer electrolyte.

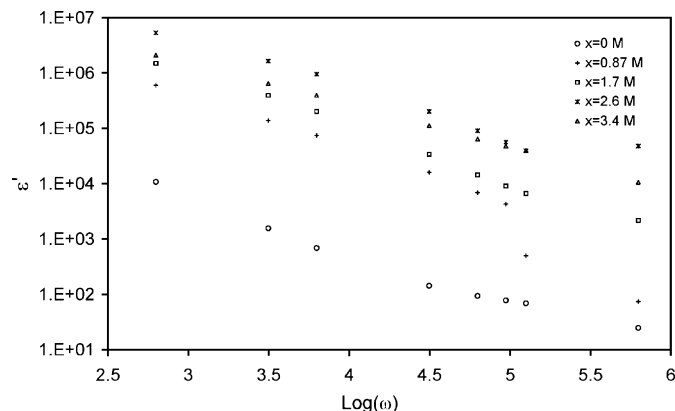


Fig. 7. Variation of dielectric constant with frequency at temperature 303 K of (PVA)<sub>0.7</sub>(NaBr)<sub>0.3</sub>:x M (SA) polymer electrolyte.

### 3.3. Dielectric studies

From Fig. 6 it is evident that dielectric permittivity increases with the increase of temperature for PVA:NaBr:x M (SA) polymer electrolyte system. The variation of  $\epsilon'$  with temperature is different for non-polar and polar polymers. In general for non-polar polymers  $\epsilon'$  is independent of temperature. But in the case of polar polymers the  $\epsilon'$  increases with the increase of temperature. This behaviour is typical of polar dielectrics in which the orientation of dipoles is facilitated with the rising temperature and thereby the permittivity is increased [14].

The frequency dependence of  $\epsilon'$  for different values of SA concentration in the (PVA)<sub>0.7</sub>(NaBr)<sub>0.3</sub> system at room temperature are shown in Fig. 7. From the plots it is clear that the permittivity decreases monotonically with increasing frequency. Similar behavior was observed in other materials [7]. This is because, for polar materials, the initial value of the dielectric permittivity is high, but as the frequency of the field is raised the value begins to drop which could be due to the dipoles not being able to follow the field variation at higher frequencies and also due to the polarization effects [14]. The low frequency dispersion region is attributed to the charge accumulation at the electrode–electrolyte interface. At higher frequencies the periodic reversal of the electric field occurs so fast that there is no excess ion diffusion in the direction of the field. Hence  $\epsilon'$  decreases with the increase of the frequency in all the samples of PVA polymer electrolytes.

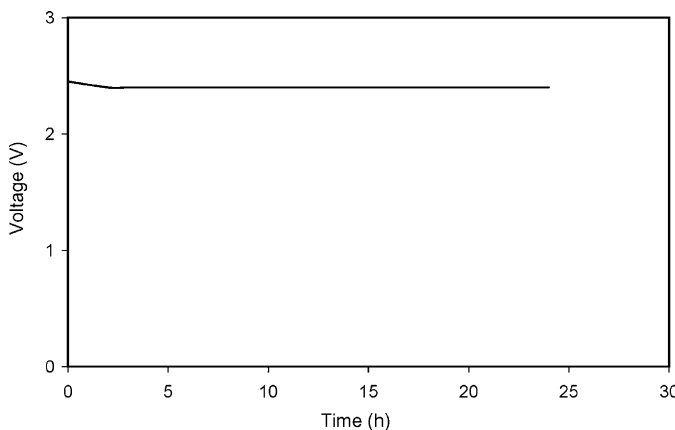


Fig. 8. Open-circuit voltage (OCV) of Mg/SPE/MnO<sub>2</sub> cell during 24 h of storage.

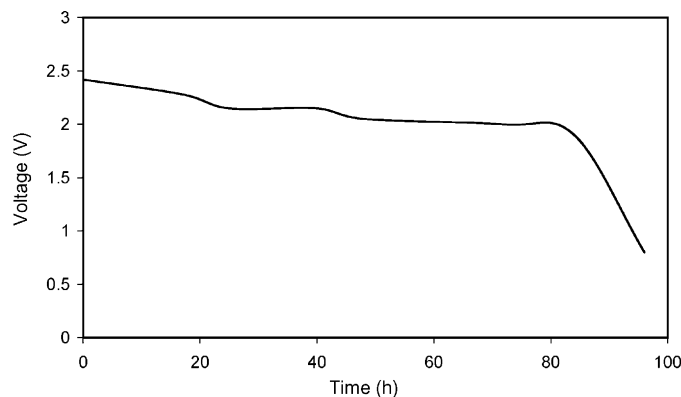


Fig. 9. Discharge characteristic for Mg/SPE/MnO<sub>2</sub> cell at a constant load of 100 kΩ.

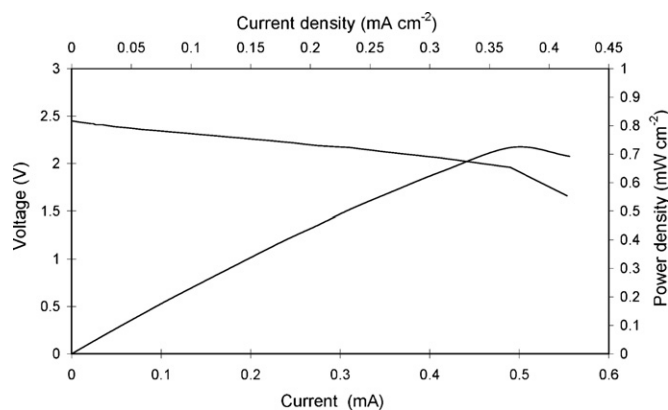


Fig. 10. *I*-*V* and *J*-*P* curves for Mg/SPE/MnO<sub>2</sub> cell.

#### 3.4. Battery characterization

The open-circuit voltage characteristic of the Mg/SPE/MnO<sub>2</sub> battery at room temperature is shown in Fig. 8. There seems to be a voltage delay at the time of assembly when the voltage was observed higher in the first 2 h and later stabilized at 2.37 V. The OCV remained constant at 2.37 V until the 24 h of storage. The OCV value obtained in the present study using PVA:NaBr:SA polymer electrolyte system was more than values documented [1]. Fig. 9 shows the discharge characteristic of the battery at a constant load  $R = 100 \text{ k}\Omega$ , which gave a flat discharge plateau at 2.22 V. It shows that the discharge voltage  $V(t)$  was sustained for 86 h until the cut-off voltage of 1.9 V. The value of the discharge capacity  $C$  was evaluated from the equation [15]:

$$C = \frac{1}{R} \int_0^t V(t) dt$$

by integrating the area under curve of Fig. 10. The discharge capacity estimated by  $4.85 \text{ mAh g}^{-1}$  for the limited electrode

(MnO<sub>2</sub>). Fig. 10 shows the *I*-*V* and *J*-*P* characteristics for the Mg/SPE/MnO<sub>2</sub> battery at room temperature. The *I*-*V* curve had a simple linear form which indicates that the polarization on the electrode was primarily dominated by ohmic contributions. The plot of the operating *J*-*P* suggests that the contact between electrolyte/electrodes was good. The voltage of the battery dropped to a short circuit current density of  $0.42 \text{ mA cm}^{-2}$  and the maximum power density was determined to be  $0.74 \text{ mW cm}^{-2}$ . The internal resistance of the battery was obtained from the gradient of the *I*-*V* graph, which was  $900 \Omega$ .

#### 4. Conclusion

The H<sub>2</sub>SO<sub>4</sub>-doped (PVA)<sub>0.7</sub>(NaBr)<sub>0.3</sub> solid polymer electrolyte was characterized physicochemically and electrochemically in this study and applied to all solid-state magnesium battery. The information obtained is summarized as follows: Electrical and electrochemical properties of (PVA)<sub>0.7</sub>(NaBr)<sub>0.3</sub> solid polymer electrolyte have been improved due to doping by sulfuric acid. The highest conducting film can be used to fabricate solid-state magnesium battery. Although, the capacity obtained is less than the theoretical value ( $308 \text{ mAh g}^{-1}$  of MnO<sub>2</sub> for one-electron reduction), the studies suggest (PVA)<sub>0.7</sub>(NaBr)<sub>0.3</sub>:SA a promising solid polymer electrolyte for magnesium cells. Further extensive investigations are required, however, to raise the performance of the magnesium-based rechargeable cells to practical levels.

#### References

- [1] Ji-Sun Oh, Jang-Myoun Ko, Ji-Sun Kim, *Electrochimica Acta* 50 (2004) 903.
- [2] Nobuko Yoshimoto, Shin Yakushiji, Masashi Ishikawa, Masayuki Morita, *Solid State Ionics* 152 (2002) 259.
- [3] Yanna NuLi, Zaiping Guo, Huakun Liu, Jun Yang, *Electrochemistry Communications* 9 (2007) 1913.
- [4] G. Hirankumar, S. Selvasekarapandian, N. Kuwata, J. Kawamura, T. Hattori, *Journal of Power Sources* 144 (2005) 262.
- [5] Soo-Kyeong Jeong, Yun-Kyung Jo, Nam-Ju Jo, *Electrochimica Acta* 52 (2006) 1549.
- [6] P. Balaji Bhargav, V. Madhu Mohan, A.K. Sharma, V.V.R.N. Rao, *Ionics* 13 (2007) 441.
- [7] A.A. Mohamad, A.K. Arof, *Materials Letters* 61 (2007) 3096.
- [8] M. Hema, S. Selvasekarapandian, A. Sakunthala, D. Arunkumar, H. Nithya, *Physica B: Condensed Matter* 403 (2008) 2740.
- [9] A. Martinelli, A. Matic, P. Jacobsson, L. Börjesson, M.A. Navarra, A. Fericola, S. Panero, B. Scrosati, *Solid State Ionics* 177 (2006) 2431.
- [10] A.A. Mohamad, N.S. Mohamed, M.Z.A. Yahya, R. Othman, S. Ramesh, Y. Alias, A.K. Arof, *Solid State Ionics* 156 (2003) 171.
- [11] S.F. Johnston, I.M. Ward, J. Cruickshank, G.R. Davies, *Solid State Ionics* 90 (1996) 39.
- [12] L.S. Ng, A.A. Mohamad, *Journal of Power Sources* 163 (2006) 382.
- [13] S. Saravanan, C. Joseph Mathai, M.R. Anantharaman, S. Venkatachalam, P.V. Prabhakaran, *Journal of Physics and Chemistry of Solids* 67 (2006) 1496.
- [14] B. Tareev, *Physics of Dielectric Materials*, MIR Publications, Moscow, 1979.
- [15] N. Cui, J.L. Lou, *Electrochimica Acta* 44 (1998) 711.